Psychophysical Measurement of Marmoset Acuity and Myopia

AQ4 **Samuel U. Nummela,**[1] **Shanna H. Coop,**[2] **Shaun L. Cloherty,**[2,3] **Chantal J. Boisvert,**[4] **Mathias Leblanc,**[5] **Jude F. Mitchell**[2]

AQ2 [1] Cortical Systems and Behavior Laboratory, University of California, San Diego

[2] Brain and Cognitive Sciences, University of Rochester, New York

[3] Department of Physiology, Monash University, Melbourne, Australia

[4] Gavin Hebert Eye Institute, University of California, Irvine, California

[5] Animal Resources Department, The Salk Institute, La Jolla, California

ABSTRACT: The common marmoset has attracted increasing interest as a model for visual neuroscience. A measurement of fundamental importance to ensure the validity of visual studies is spatial acuity. The marmoset has excellent acuity that has been reported at the fovea to be nearly half that of the human (Ordy and Samorajski [1968]: Vision Res 8:1205–1225), a value that is consistent with them having similar photoreceptor densities combined with their smaller eye size (Troilo et al. [2000b]: Vision Res 33:1301–1310). Of interest, the marmoset exhibits a higher proportion of cones than rods in peripheral vision than human or macaque, which in principle could endow them with better peripheral acuity depending on how those signals are pooled in subsequent processing. Here, we introduce a simple behavioral paradigm to measure acuity and then test how acuity in the marmoset scales with eccentricity. We trained subjects to fixate a central point and detect a peripheral Gabor by making a saccade to its location. First, we found that accurate assessment of acuity required correction for myopia in all adult subjects. This is an important point because marmosets raised in laboratory conditions often have mild to severe myopia (Graham and Judge [1999]: Vision Res 39:177–187), a finding that we confirm, and that would limit their utility for studies of vision if uncorrected. With corrected vision, we found that their acuity scales with eccentricity similar to that of humans and macaques, having roughly half the value of the human and with no clear departure for higher acuity in the periphery.   © 2016 Wiley Periodicals, Inc. Develop Neurobiol 00: 000–000, 2016

Keywords: marmoset; vision; myopia; psychophysics

INTRODUCTION

The common marmoset (*Calithrix jacchus*) is a small bodied New World monkey which offers an interesting point of comparison between mice and macaques in the study of vision (Mitchell and Leopold, 2015). Like macaques, marmosets have a specialized fovea with comparably high cone density that drops with retinal eccentricity (Troilo et al., 1993) and show a

1

2   *Nummela et al.*

similar cortical magnification factor in primary visual cortex (Chaplin et al., 2013). They can also be trained to perform basic visual tasks when head-fixed, which is crucial for precise eye tracking and many standard electrophysiological techniques (Mitchell et al., 2014b). However, many important facets of marmoset vision remain unknown compared to the better studied macaque model for vision.

One crucial feature of vision is acuity, which determines which visual features can be seen, and thus specifies the range of appropriate visual stimuli for future studies. One early study reported a peak visual acuity of 30 cycles per degree for marmosets (Ordy and Samorajski, 1968), about half that of humans and macaques. This result is consistent with the similarity in peak cone densities of marmosets to humans and macaques, with the half fold reduction in acuity being accounted for by their eyes being about half the size (Troilo et al., 1993). The retinal cone density in the marmoset also has one interesting difference from humans and macaques. It does not drop as rapidly at peripheral eccentricities that are beyond 5–10 visual degrees (Troilo et al., 1993; Goodchild et al., 1996; Wilder et al., 1996). This change in peripheral cone density, however, does not appear to impact the receptive field properties at the level of primary visual cortex where the cortical magnification factor is highly similar for the marmoset as for humans and macaques (Chaplin et al., 2013). A lower resolution for receptive fields in visual cortex, and for visual perception, than the resolution of photoreceptors could be explained by how the photoreceptors are pooled for further visual processing. Indeed, there is evidence of greater convergence from cone photoreceptors onto retinal ganglion cells at more peripheral retinal eccentricities (Goodchild et al., 1996), which could offset any gains in acuity based only on the photoreceptor density. In this article, we measure acuity thresholds as a function of retinal eccentricity using modern behavioral techniques to determine how differences in cone density might impact acuity in the marmoset. These behavioral measurements are also fundamental for continuing vision research to select appropriate stimuli across the range of eccentricities typically used in neurophysiological and psychophysical tasks.

To make accurate measurements of acuity, we found that it was first necessary to correct the refractive optics of the marmoset eyes. This is an important point because those studies that wish to study their normal visual processing, for example, to examine their interest in social stimuli such as faces (Mitchell et al., 2014b; Miller et al., 2016), must first consider which features of the stimuli can be resolved at the

distance they are displayed. It has been appreciated for some time that marmosets raised in laboratory lighting and viewing conditions are typically near-sighted, exhibiting myopia requiring -1 to -3 diopters spherical correction (Graham and Judge, 1999), and that the development of the marmoset eye is particularly sensitive to visual deprivation, which may explain the prevalence myopia (Troilo and Judge, 1993). Indeed, the marmoset has played a leading role as a developmental model of eye growth and understanding how blur and defocus provide visual signals that contribute to correction of refractive state over development (Troilo and Judge, 1993; Rada et al., 2000; Troilo et al., 2000a,b; Whatham and Judge, 2001; Nickla et al., 2002; Troilo and Nickla, 2005; Troilo et al., 2006; Troilo et al., 2007; Benavente-Perez et al., 2012). Whereas marmosets in their natural state may receive appropriate signals to guide their eye growth, our findings confirm that when raised in laboratory settings they exhibit mild to severe myopia which must be corrected to optimize studies of vision.

After correcting for refractive error, we examined the spatial acuity of two mature marmosets as a function of retinal eccentricity. We developed a simple grating detection task that can be used as a diagnostic to measure acuity and also to determine if a subject requires correction for distance vision. Additionally, we tested parafoveal and near peripheral eccentricities where marmosets are reported to have higher cone densities than humans or macaques.

METHODS

Subjects and Surgery

Two adult common marmosets (*Calithrix jacchus*) served as subjects M and S for experiments to correct vision and to collect corrected vision spatial frequency thresholds. Three additional adult marmosets, B, K, and, P served as subjects to collect spatial frequency thresholds in the absence of corrected vision. B, M, P, and S were male; K was female. All experiments were approved by the Institutional Animal Care and Use Committees at their respective institutions (M and S at the University of Rochester, New York; B, P, and K at the University of California, San Diego).

The viewing and lighting conditions during visual development can impact the quality of marmoset refractive state and visual acuity at maturity (Graham and Judge, 1999; Smith et al., 2012). Subjects M, B, K, and P were raised among their family groups of 4–6 members inside a laboratory setting with an enriched habitat for climbing with typical viewing distances of 3–5 feet and standard indoor fluorescent lamps (< 500 lux). Subject S was raised at a

Developmental Neurobiology

national primate center. All animals were raised in larger family groups and then pair-housed at maturity.

For several weeks prior to surgery, subjects were acclimated to sit calmly in a small primate chair following methods previously described (Lu et al. 2001; Remington et al. 2012; Osmanski et al. 2013). The design of the primate chair includes a slot that allows the marmoset's tail to hang freely with their weight lifted off their hind quarters, supporting themselves by pressing their lower legs against the inside of the small body tube in which they sit (tube diameter 3 to 3.5 inches). Animals were trained for 2–3 months to sit calmly in the chair without struggle for an extended period, beginning with short intervals of 5 min and building toward a total period of 30–60 min.

All subjects underwent surgery to implant an acrylic head cap with a titanium post that was used to stabilize the head (Lu et al. 2001). The implant surgery was performed under sterile conditions. Animals were first anesthetized using an induction chamber with isoflurane, then given IM injections of Ketamine (5–15 mg/kg), Midazolam (0.25 mg/kg), and Dexmedetomidine (0.02–0.1 mg/kg). Animals were intubated with an endotracheal tube and placed on isoflurane gas at a rate of 0.5–3% to obtain deep anesthesia. Surgeries were performed in a stereotax following standard procedures to dissect the scalp, insert bone screws, and build an acrylic cap to hold the head-post in place. After dissection, special care was taken to remove all periosteum and tissue from skull, while dilute hydrogen peroxide (1.5%) was used to clean the skull. Eight titanium screws (Synthes, 6 mm length and 1.5 mm diameter) were placed on the skull to a depth greater than 1 mm but less than 1.5 mm, and a coat of Copalite dental varnish was applied to the dried surface of the skull. A small ring of C&B-Metabond (Parkell) adhesive dental cement, was formed around the perimeter of the exposed skull to deter growth of granulation tissue into the implant. Clear fMRI compatible dental acrylic (Ortho-Jet, Lang Dental Manufacturing Co) was used to attach the head post and then applied over many successive small layers until the skull screws were covered. Once the implant was formed, the wound margin was flushed with sterile saline and the edges of the skin were glued to the base of the implant using VetBond (3M).

Following surgery animals were monitored daily for a period of 1–2 weeks and bandages were applied to cover the wound margin as needed to ensure it remained clean. During this initial period head restraint was limited to manually holding to minimize the stress on the implant. Subjects were also separated from their cage partner in an adjacent cage compartment to prevent them from tampering with the wound margin during healing. Once the skin sealed around the implant, the subject was reintroduced to their partner and normal grooming resumed with no bandages. Three weeks following the surgery chair conditioning began with head-restraint, first by manually holding the head-post and providing treats, followed after a week by mechanical restraint in a holder described previously (Remington et al., 2012). As marmosets acclimated to

mechanical restraint, we introduced reward with juice delivery through a tube (20 gauge) fixed to a 1 mL syringe, connected by plastic tubing to a 20 mL syringe in a syringe pump (NE-500, New Era Pump Systems). The juice tube was carefully positioned from the side of the animal with its tip pressing just below the upper lip and making no contact with teeth. This positioning allows juice to drip into the mouth and prevents the liquid from splashing towards the eye. Marmosets were acclimated to head-fixing for 1–2 weeks as intermittent drops of juice were delivered while viewing natural images on a display.

After recovery and chair acclimation, animals were trained to maintain fixation on a small point using methods for eye tracking under head-restraint described previously (Mitchell et al., 2014b). Subjects B, M, and S were food scheduled with free access to water to encourage motivation during the behavioral tasks. The daily food allotment was gradually lowered until subjects reached 85–90% of their normal (free feed) weights.

Behavioral Task

Acuity was measured using a Gabor detection task. Figure 1(A) provides example sequence of events for a correct trial (top) and an incorrect trial (bottom). The task was initiated by fixation of a small spot (0.25 degree radius, 0.5 cd/m^2 center, 230 cd/m^2 surround) for a delay uniformly distributed between 0.2 to 0.5 s, presented on a gray background (115 cd/m^2). Fixation was maintained within a 0.75 to 1.5 degree radius window centered on the spot. On completing this fixation period, a vertically oriented Gabor appeared for 0.3 s (peak 230 cd/m^2, trough 0.5 cd/m^2) with a concurrent dimming of the fixation spot (70 cd/m^2 center, 161 cd/m^2 surround). Within each behavioral session, the Gabor could appear at one of eight locations surrounding the fixation spot. After the Gabor presentation, both fixation spot and Gabor were replaced by four equally spaced low contrast rings (110 cd/m^2) indicating possible locations that the Gabor could have appeared; this was done to encourage a saccadic choice. From the onset of Gabor, the subject was given up to 1.5 s to make a saccade out of the fixation window toward one of the rings, if the saccade landed toward the ring where the Gabor had appeared (a pie slice within pi/5 radian angle of the target center). Eye position needed to remain in the correct window for 0.25 s to confirm the saccade endpoint. A correct choice [Fig. 1(A), top] was rewarded with a 10–20 μL liquid reward and the appearance of a marmoset face at the Gabor location for 1 s, providing positive feedback. The juice reward consisted of marshmallows blended with water that were prepared fresh for each daily session (2 large, 60 g, marshmallows blended in 30 mL hot water, left to settle for a few minutes, then the lower portion drawn into a 20 cc syringe). An incorrect choice [Fig. 1(A), bottom] resulted in the correct ring location increasing in contrast (68 cd/m^2), and reappearance of the Gabor stimulus for 1 s to provide feedback for where the saccade should have been directed. In either case the next trial proceeded after a 2 s interval.

F1

4 *Nummela et al.*
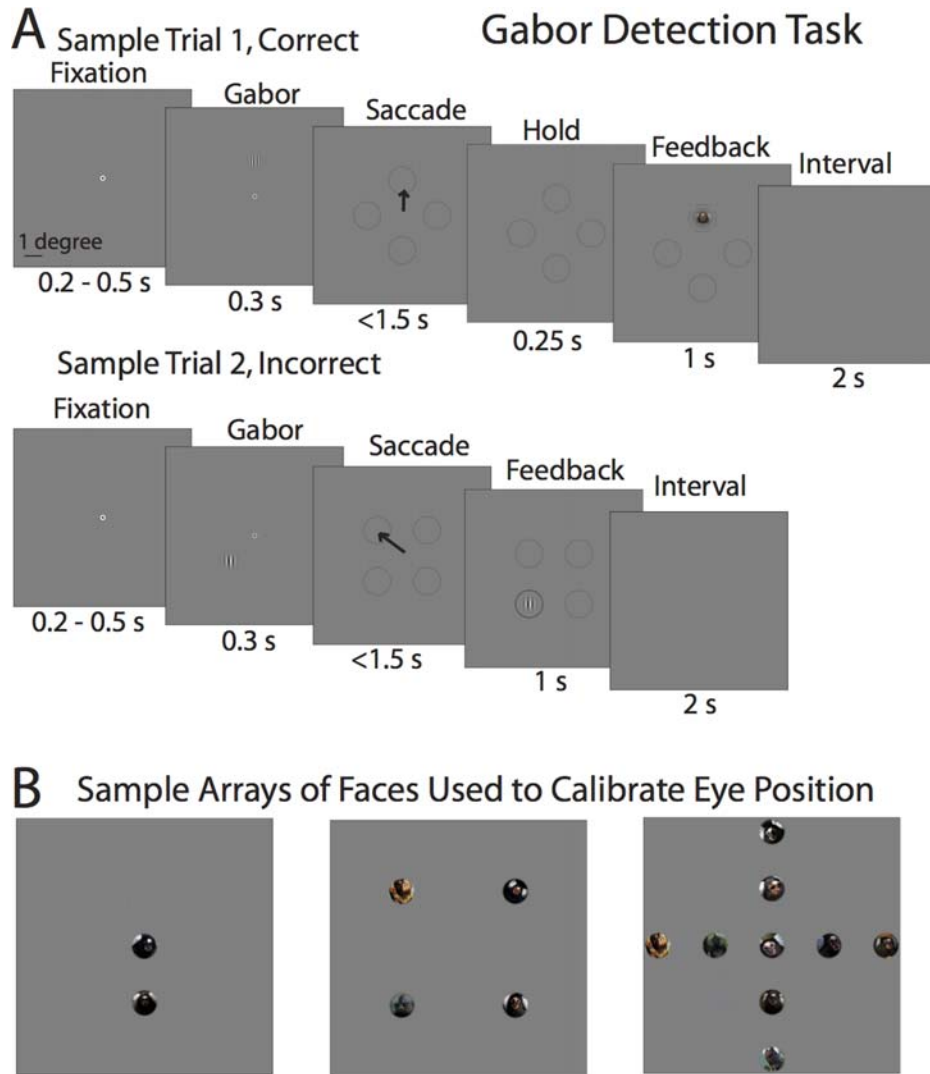
Figure 1 Behavioral tasks. (A) A series of frame shots illustrating two sample trials of the Gabor detection task, one correct trial (above) and one incorrect trial (below). Briefly, the animal was required to fixate a small central spot for 0.2 to 0.5 s, after which a Gabor was presented for 0.3 s, followed by four possible choice rings and the offset of the fixation spot. The animal was required to make a saccade within 1.5 s of the Gabor onset (and could be made before choice rings appeared). A saccade toward the Gabor location had to be held for 0.25 s to earn a liquid reward and marmoset face image before the next trial. If the saccade was directed to an incorrect location the Gabor reappeared with a higher contrast ring at the correct location to provide feedback. In either case a 2 s interval preceded the next trial. The scale bar in the fixation panel and arrows in the saccade panels indicate visual scale and saccadic choices, and were not present on the visual display. (B) Sample arrays of faces superimposed with eye position traces, used to calibrate eye position. Because marmosets unpredictably redirect gaze away from a single face, an array of faces keeps the marmoset gaze directed at several known points in visual space throughout eye calibration.

The Gabor stimulus was always vertically oriented; however spatial frequency and Gabor location was pseudo-randomized over a trials list to construct a psychometric function of spatial frequency sensitivity using the method of constant stimuli. The phase of the Gabor was randomized on each trial.

Within a behavioral session, the eccentricity and size of the Gabor was fixed, however this could vary from session to session (see Table 1, which details conditions of the Gabor task for measurement of acuity for subjects M and S). We tested acuity across a range of values (1.5, 2, 3, 4, 5, 6, 7, 8, 10, and 12 degrees). The order of eccentricity values

T1

Developmental Neurobiology

Table 1 Task Parameters for Acuity Measurement

Subject [Diopter]	Gabor Eccentricity (Degrees)	Gabor Sigma: Fixed/ Varying (Degrees)	Gabor Spatial Frequency: Low to High (c/deg)	Display Distance (cm)
M [-3.5]	1.5	0.25/0.06	7.0 to 16.5	90
	2	0.25/0.13	7.0 to 15.0	90
	3	0.25/0.19	5.5 to 13.5	90
	4	0.25/0.25	5.5 to 12.5	90
	5	0.25/0.31	4.5 to 12.0	90
	6	0.25/0.38	3.5 to 11.0	90
	7	0.25/0.44	3.0 to 11.5	90
	8	0.25/0.50	2.5 to 12.0	90
	10	0.25/0.63	1.5 to 9.0	49
	12	0.25/0.75	0.5 to 8.0	49
S [-2.0]	2	—/0.13	8.3 to 15.5	90
	3	—/0.19	7.5 to 15.5	90
	4	—/0.25	6.0 to 15.5	90
	5	—/0.31	7.0 to 15.5	90
	6	—/0.38	6.5 to 13.5	90
	7	—/0.44	4.3 to 12.5	90
	8	—/0.50	5.0 to 12.0	90
	10	—/0.63	2.5 to 11.0	49
	12	—/0.75	3.0 to 12.0	49

tested was pseudo-randomized across sessions with each value being tested at least twice in a separate behavioral session, such that each value was tested in the first half of sessions and then again in the second half of sessions (to reduce any potential training effects). In subject M, we performed tests of two eccentricities each day in a back to back session. In this subject the tested eccentricities were swapped during the collection of the second half of sessions to counter any fatigue effects due to the order of presentation each day. We measured lapse rates to ensure that fatigue and long term training effects did not contribute to any systematic bias in our measurements.

Eyes were calibrated each day prior to Gabor detection task sessions by presenting arrays of marmoset faces as described previously (Mitchell et al., 2014b). Example arrays of faces are shown in Figure 1(B). Horizontal and vertical eye position and gain parameters were manually adjusted on-line until eye position fixations matched the positions of the faces in the arrays. Eye position of central gaze was subsequently fine-tuned using a small fixation spot (0.25 degree radius, 0.5 cd/m^2 center, 230 cd/m^2 surround) on a gray background (130 cd/m^2) and rewarding the marmoset for maintaining fixation within a large fixation window (2 degree radius) for 0.5 to 1.5 s.

Our visual display backgrounds were set to 115 cd/m^2. This was done for two reasons. First, it ensured our measurements of acuity were mediated by cones, and not a combination of cones and rods (Freitag and Pessoa, 2012). Second, this level of brightness shrinks the marmoset pupil diameter, allowing for easier measurement of eye position using video eye tracking.

Hardware and Software

Stimuli were presented on a 2.2 gamma corrected LED display (X2411z, BenQ) in 1080p, which had a dynamic range from 0.5 to 230 cd/m^2. Brightness on the display was set to 100 and contrast to 50, and additional visual features of the monitor such as blur reduction and low blue light were turned off. For one experiment, a gamma corrected iPad Air 2 (Apple) running the Duet Display application was used as a visual display to provide greater pixel resolution for high frequency Gabors at short viewing distances (dynamic range of 0.35 to 330 cd/m^2). Gamma corrections were verified with measurement by a photometer. All Gabor and fixation stimuli were presented in grayscale, face rewards and faces for calibrating eye position were presented in color. To accommodate sufficient resolution for Gabors at eccentricities near the fovea, and sufficient space to present stimuli at eccentricities further away, the display was moved between 29 cm and 150 cm distance from the marmoset subject, but it was typically placed at 90 cm.

Eye position was acquired at 220 Hz using an Eye Tracker and Viewpoint software (Arrington Research), with eye position collected from infrared light reflected off of a dichroic mirror (part #64-472, Edmunds Optics). When applying visual correction, spherical concave lenses (Optimark Perimeter Lens Set) were centered 4–5 mm in front of the animal's face, which introduces minimal artifacts. This lens distance minimally weakens the diopter strength (e.g., the −3.50 diopters lens for Subject M corrects for −3.45 diopters at 5 mm distance) and induces a small base out prism diopter of 0.5 for the average inter pupillary distance of 13 mm, which can be accommodated, and is not expected to affect acuity. Eye calibration and Gabor detection tasks were controlled using a custom Matlab GUI on a Windows 7 machine with Intel i7 cpu, 8 GB RAM, and GeForce Ti graphics card, which was presented on a second display. The software subsampled eye position on-line at

Developmental Neurobiology

6   *Nummela et al.*

the display refresh rate of 120 Hz using the ViewPoint Matlab toolbox (Arrington) and presented visual stimuli using the PsychoPhysics Toolbox (Brainard, 1997; Pelli, 1997; Kleiner et al., 2007). Use of a photodiode (SD200-12-22-041-ND, Digi-Key) confirmed that the Matlab GUI did not affect the timing of frame flips at the task display refresh rate of 120 Hz.

Acuity Threshold Calculation

All analyses were performed using Matlab 2014b (Mathworks) and the Palamedes toolbox (Prins and Kingdom, 2009, www.palamedestoolbox.org). Acuity thresholds in cycles per degree were calculated for Gabors presented at each eccentricity by fitting psychometric curves. For the demonstration of visual correction, acuity thresholds were calculated within a single eccentricity of 4 degrees for different spherical corrections. For each psychometric curve, all trials at each spatial frequency were pooled, and fraction correct and confidence intervals calculated using the "binofit" function. Spatial frequencies were collected in a range that varied from a value low enough to exceed 75% correct performance to a value high enough that performance was not significantly different from chance, 25%. These points were fit with a four parameter logistic function using the Palamedes function "PAL_PFML_Fit," where two free parameters, alpha and beta, determined the shape of the logistic function, and two restricted parameters, gamma and lambda, determined the lower bound of the logistic function (fixed at chance performance of 25% correct trials) and the lapse rate (restricted to be between 0 and 0.5), respectively. Acuity threshold was estimated from the point of the logistic psychometric fit that was half way between gamma, chance performance, and 1-lambda, the lapse rate. Confidence intervals for threshold were constructed by 400 bootstraps of the logistic fit using the "PAL_PFML_ BootstrapNonparametric" function.

Ophthalmological Examination and Refraction

Subjects M, S, P, and B underwent ophthalmologic refraction under anesthesia to confirm they were near-sighted. This procedure was performed by an experienced ophthalmologist (CJB). One drop of 1% tropicamide and 2.5% phenylephrine hydrochloride were given twice 5 min apart 30 min prior to the examination to induce cycloplegia and pupillary dilation. Eyelids were manually opened and corneas were irrigated with sterile saline. Cycloplegic refraction with a streak retinoscope and handheld trial lenses was performed. Measurements were obtained at a 50-cm working distance, and the refractions of the most plus and most minus meridians were recorded in the plus cylinder form. The anterior segment examination was performed using a Finoff ocular transilluminator, and a direct ophthalmoscope was used to evaluate the clarity of the red reflex by retroillumination. The fundi were evaluated by using an indirect ophthalmoscope and a Panretinal 2.2 lens (Volk Optical,

Table 2   Visual Corrections by Subject

Subject	Behavioral Correction	Ophthalmological Correction
M	−3.50	OD −2.50/+0.50 × 90
		OS −2.50
S	−2.00	OD −2.50/+1.00 × 90
		OS −2.00
B	No Data	OD −2.00/+2.00 × 90
		OS −2.00/+2.00 × 90
P	No Data	OD −3.50/+0.50 × 90
		OS −3.50/+0.50 × 180
K	No Data	No Data

Mentor, OH). Measurements for each subject are provided in Table 2, including spherical correction and astigmatism.   T2

RESULTS

The importance of correcting for refractive state in vision studies with captive raised marmosets cannot be understated. Though marmosets raised in the wild could have a low incidence of myopia (near-sightedness), the reported values for those raised in laboratory settings is high (Graham and Judge, 1999), findings that are confirmed in our own small sample of subjects. Our initial attempts to measure acuity (subjects B, K, and P), without first correcting for refractive state, revealed a highly unusual pattern for the spatial frequency threshold as we brought stimuli closer to the fixation point. Instead of a continued rise in the acuity threshold nearing the fovea (as predicted by the sharp increase in retinal cone density, see Troilo et al., 1993, Fig. 4), we observed a flattening of the threshold. This flattening of threshold can be explained by the low-pass filter properties of distance vision if the subject is myopic. Our method of testing was particularly susceptible to myopia because we varied monitor distance to provide adequate pixel sampling of high spatial frequency stimuli. For stimuli near fixation, the visual display was placed at distances of 90 cm or more, which impairs measurement of acuity for animals suffering from mild myopia, anything greater than −1.25 diopters. After ophthalmological refraction of the eyes of subjects B and P (Table 2), we were able to confirm that they were indeed near-sighted, requiring spherical diopter corrections of −2.00D and −3.50D. Although the summary data for these subjects will be presented later to demonstrate the deficits caused by uncorrected vision, we begin the results section by characterizing and correcting for the visual deficits of subjects M and S.   F4

AQ1

We developed a simple behavioral diagnostic to identify marmoset subjects with myopia. Using the Gabor detection task previously described (see methods), we first determined the acuity threshold of each subject with uncorrected vision at a fixed eccentricity, but varying the distance of the visual display. The eccentricity (4 visual degrees) and size of the stimulus (1.5 visual degrees radius) was maintained constant by scaling stimuli on the display as the display distance varied. A decline in spatial frequency sensitivity as the distance increases indicates myopia, whereas no change is expected from a subject with perfect vision. Figure 2(A) illustrates how we measured these spatial frequency thresholds at each distance for subject M. Each plot in Figure 2(A) shows the fraction of correct trials for every spatial frequency tested at one visual display distance. The performance at each distance was then fit to a logistic psychometric curve as described in methods. The psychometric curves for each plot in Figure 2(A) are shown overlaying the raw data, and are characterized by a rapid transition from the upper bound across the spatial frequency threshold to the lower bound. For subject M, this transition occurs above 7.5 cycles per degree at a display distance of 29 and below 7.5 cycles per degree at 90 cm, indicating a decrease in spatial frequency sensitivity with distance. We defined threshold as the spatial frequency corresponding to the midpoint between upper and lower bounds of the psychometric curve. This was done to minimize the influence of the lapse rate, which determines the upper bound of the psychometric curve, and could vary from session to session, on threshold measurements.

F2

The effects of visual display distance on spatial frequency sensitivity are summarized for subjects M and S [Fig. 2(B)]. For subject M (shown in blue), spatial frequency threshold consistently declined with increasing distance ($r = -0.93$, $p = 0.02$), with a net decrease of 2.5 cycles per degree, or about 30%, from 29 cm to 90 cm ($p < 0.01$, bootstrap). In contrast to subject M, subject S (shown in green) showed much less severe declines in spatial frequency threshold ($r = -0.64$, $p = 0.24$). Part of this pattern reflects the superior distance vision of this subject, reflected by the higher overall uncorrected acuity than subject M, but it also reflects a complication due to display resolution that we consider in more depth.

A key limitation in measuring acuity, particularly for near distances, is the pixel resolution in conventional displays for showing grating stimuli without aliasing or loss of contrast. Notably, the pattern in subject S did not show a consistent increase in spatial frequency threshold as the display was brought closer, as would be expected for a near-sighted subject. This likely reflects distortion of the Gabor stimuli at near distances due to limitations of the visual display resolution, with only 2 pixels per Gabor cycle at 11.5 cycles per degree when shown at the closest distance tested (29 cm). As the display approaches this resolution limit, subsampling introduces higher spatial frequencies and reduces the contrast of the intended spatial frequency, making threshold measurements unreliable. To test if inadequate Gabor sampling was limiting performance in subject S, we used an iPad to collect data at 29, 36, and 49 cm [Fig. 2(B), brown markers]. This provided a minimum of 4 pixels per cycle for spatial frequencies below 16 cycles per degree at 29 cm. With increased display resolution, the spatial frequency threshold of subject S at 29 cm increased by 1.3 cycles per degree ($p < 0.01$, bootstrap), and was also 2 cycles per degree higher than the threshold measured at 90 cm ($p < 0.01$, bootstrap). Replacement of the initial subject S threshold measurements from 29 to 49 cm with the iPad measurements revealed a decline in spatial frequency sensitivity with display distance ($r = -0.90$, $p = 0.04$) that, like subject M, was consistent with myopia, though milder in form. Thus both subjects showed a presence of myopia requiring correction to measure spatial frequency sensitivity. All data presented in the rest of this article had a minimum display resolution of 4 pixels per cycle for Gabor stimuli.

To establish a minimal correction of the myopia in subjects M and S, we continued behavioral testing while introducing a spherical lens correction. We tested at the same fixed eccentricity of 4 degrees, but varied the spherical correction from plano to higher near-sighted values until performance peaked and began to flatten or decline. For each behavioral session, the stimuli were fixed at a far distance of 90 cm and a different spherical lens was placed in front of the entire face, providing the same correction to both eyes. Ideally, we might correct vision in both eyes independently; however, this would require custom design of smaller lenses fit to the marmoset, and correction with a single lens is possible using a standard lens set (see methods). Figure 2(C) demonstrates the change in performance for subject M from uncorrected vision (left) to a correction of -3.50 diopters (right). This visual correction shifts the psychometric curve from a threshold below 7.5 cycles per degree to a value above that is nearly doubled. Figure 2(D) shows the spatial frequency threshold for subjects M (blue) and S (green) as a function of diopter strength. The estimated correction was determined behaviorally, by the lens with the highest acuity, or alternatively

8 *Nummela et al.*

C
O
L
O
R
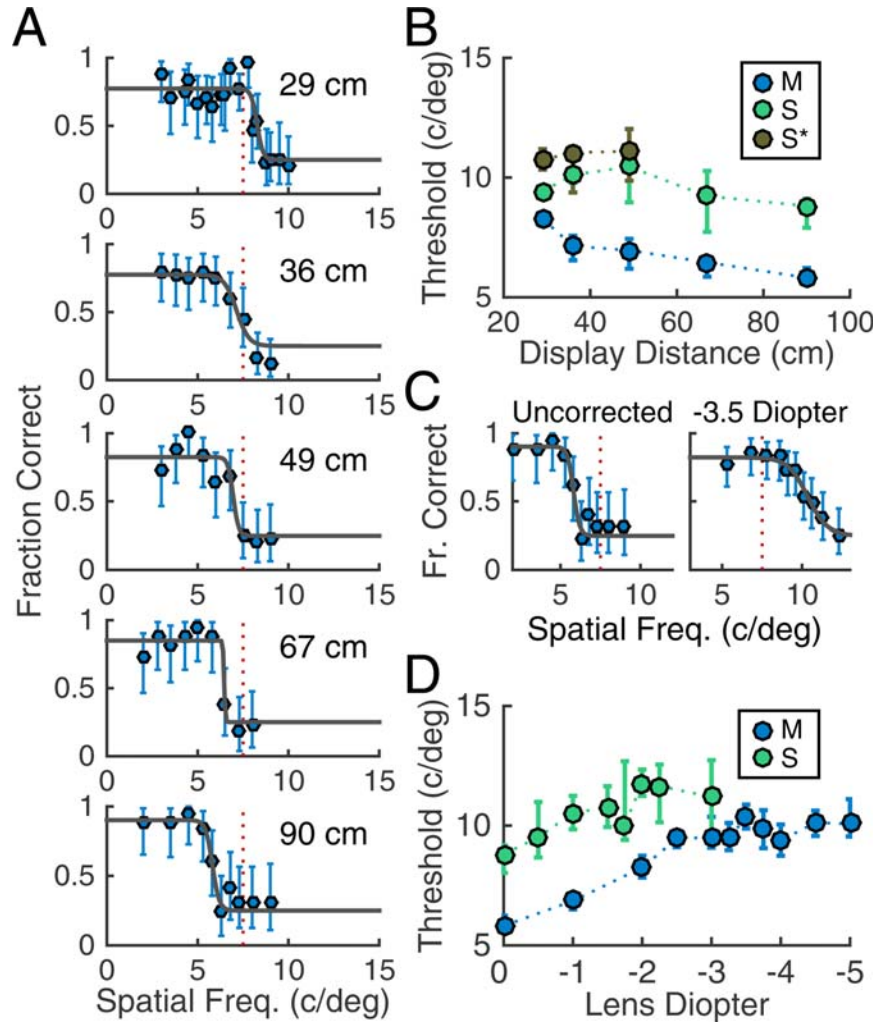
Figure 2 Correction of marmoset vision. (A) Plots of the fraction of the detected Gabor stimuli at each spatial frequency sampled, with 95% CIs, for subject M. Display distance is noted by text in each plot. Psychometric fits used to calculate spatial frequency threshold are overlaid as a solid dark gray line. Dotted red reference lines at 7.5 cycles per degree are provided to help compare psychometric fits across plots. (B) Spatial frequency sensitivities as a function of display distance for subjects M (blue) and S (green) are provided by plotting spatial frequency threshold as a function of display distance with 95% CIs from a nonparametric bootstrap. At closer display distances, subject S was also run on an iPad display to increase screen resolution (Brown, denoted S*). (C) A comparison of Gabor detection performance with uncorrected vision (left) and a −3.5 diopter correction (right) for subject M. Raw performance at each spatial frequency with 95% CIs is plotted along with psychometric fits overlaid (solid dark gray lines). A dark grey psychometric fits and a dotted red reference line. Dotted red reference lines are provided at 7.5 cycles per degree. (D) Spatial frequency sensitivities as a function of diopter correction strength at a fixed display distance (90 cm) and retinal eccentricity (4 visual degrees) are summarized for subjects M (blue) and S (green). Error bars are 95% CIs.

for curves that became flat past over-correcting, with the smallest correction giving the same highest performance. We set the correction to −3.50 diopters for subject M, which was a slight over correction from ophthalmologic measurement in Table 2, and −2.00 diopters for subject S, very close to the
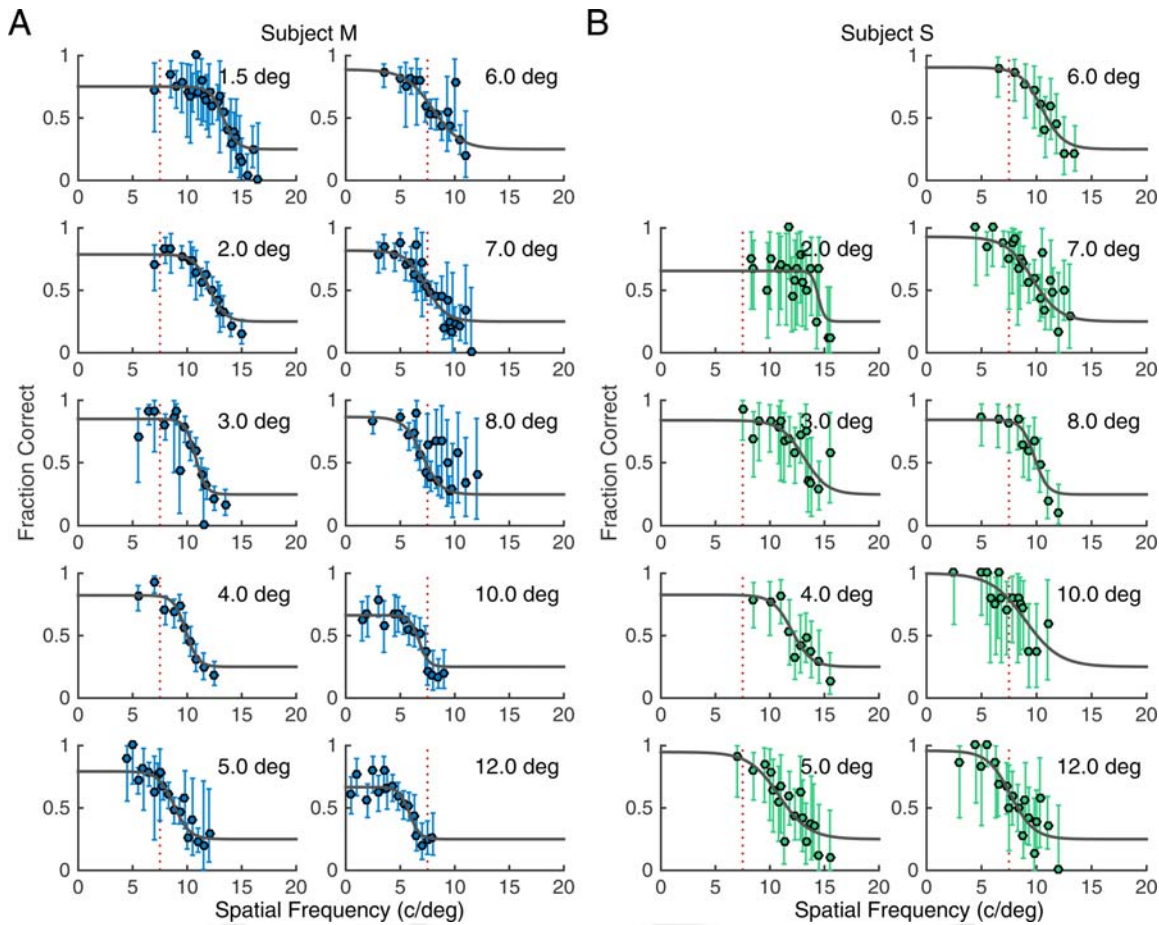
ophthalmologic measurement. Figure 2(D) also illustrates that this improvement in spatial frequency sensitivity can be very large, even at display distances of less than 100 cm. The threshold for subject M nearly doubled and increased by about 50% for subject S.

Developmental Neurobiology

Figure 3 Spatial frequency sensitivities from 1.5 to 12 degrees of visual angle. Raw data for the fraction of correct Gabor detections at each spatial frequency is provided at each eccentricity tested for subjects M (A) and S (B), each with corrected vision. Fraction correct at each eccentricity is given by the colored circles with 95% CIs. Solid dark gray lines show the psychometric fits. Dotted red reference lines at 7.5 cycles/degree provide a stable point to compare the spatial frequency thresholds measured across retinal eccentricities.

With corrected vision, we measured spatial frequency sensitivities at retinal eccentricities ranging from 1.5 to 12 degrees in subject M [Fig. 3(A)] and 2 to 12 degrees in subject S [Fig. 3(B)]. For each measurement, we plotted the raw data of fraction correct at each spatial frequency tested, and overlaid the psychometric fits. Individual data points show 95% confidence intervals of binomial distributions in which magnitude scales with the number of observations, resulting in smaller error bars for greater numbers of observations. The psychometric thresholds for both subjects shift toward lower spatial frequencies as eccentricity increases. The logistic psychometric curve weighs the number of observations at each eccentricity, which is taken into account by the nonparametric bootstrap when generating 95% confidence intervals for thresholds. Spatial frequency thresholds as a function of Gabor retinal eccentricity

are summarized in Figure 4(A) for subjects M and S with corrected vision (large circles), and also for subjects B, K, and P with uncorrected vision (small circles). All subjects exhibited an overall increase in spatial frequency threshold with decreasing retinal eccentricity ($r < -0.9$, $p < 0.05$), however both subjects with corrected vision, M and S, showed increases in spatial frequency sensitivity within 2 degrees of retinal eccentricity ($p < 0.05$, bootstrap) while subject B and P level off in that range ($p > 0.05$). Additionally, both subjects with corrected vision show significantly greater spatial acuity than subjects without corrected vision across all comparable retinal eccentricities ($p < 0.05$, bootstrap comparisons of thresholds at closest eccentricities). One concern is that more peripheral locations may require localized correction (Wang et al., 1997), especially at larger eccentricities of 20 or 30 visual degrees. For

C
O
L
O
R
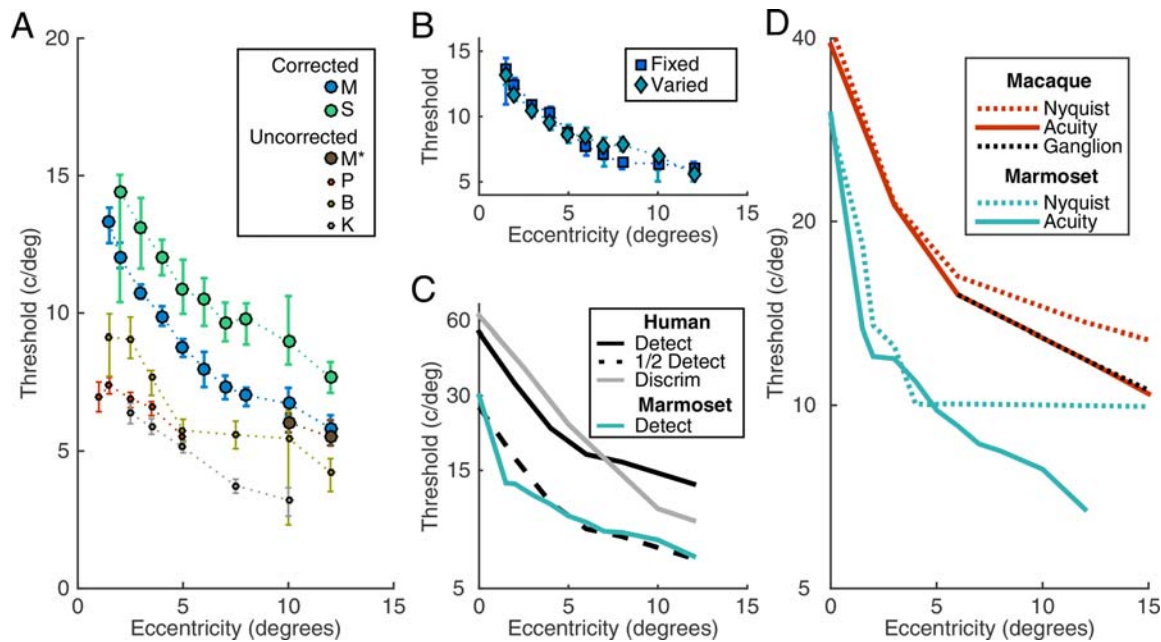
Figure 4 Acuity as a function of retinal eccentricity. Spatial frequency thresholds are summarized as a function of retinal eccentricity for all marmoset subjects. Subjects M and S were visually corrected, subjects B, K, and P were not visually corrected and exhibited myopia. M* shows data from subject M uncorrected with a very near display distance of 20 cm (close enough to not require correction). Error bars are 95% confidence intervals constructed with a nonparametric bootstrap. (B) A plot of spatial frequency sensitivity for subject M with a fixed Gabor size and a Gabor size that scaled with eccentricity. Error bars are 95% confidence intervals constructed with a nonparametric bootstrap. (C) Psychophysical measurements of human and marmoset acuity are compared. The human detection acuity curve (detect) was taken from Berkley et al., 1975, and the human discrimination (discrim) acuity curve was taken from Thibos et al., 1996. The marmoset curve was constructed by averaging the acuities of subjects M and S and using the estimate from Ordy and Samorajski, 1968. Spatial frequency thresholds are placed on a log scale to accommodate the differences between species. (D) Comparison of psychophysical measurements of acuity to theoretical limits based on retinal cell densities in macaques and marmosets. For the macaque the measurement of acuity, the theoretical acuity limit based on cone densities (Nyquist limit), and a theoretical acuity limit based on the density of P on and off retinal ganglion cells are taken from Merigan and Katz, 1990. For the marmoset, the psychophysical measurement of acuity is the same as in (C) and the Nyquist limit is taken from Troilo et al., 1993. Spatial frequency thresholds are placed on a log scale to accommodate the differences between species.

this reason, we repeated our measurements of acuity thresholds for subject M at 10 and 12 degrees eccentricity, without correction at a display distance of only 20 cm (close enough to remain in focus for myopia requiring −5 diopter correction). These measurements of acuity threshold were nearly identical to those with correction [Fig. 4(A), subject M*], suggesting that use of the same correction at all eccentricities had no adverse effect on our estimates at the most peripheral locations tested.

In subject M, we further examined to what extent varying the size of the test stimulus influenced performance and found it had minimal influence on threshold. Most of our measurements used stimuli that scaled in size with increasing eccentricity, with the

stimulus diameter fixed at 25% of the eccentricity. In subject M, we additionally repeated all measurements with a fixed stimulus size of 1 degree diameter at all eccentricities. Figure 4(B) separates spatial frequency measurements for subject M for Gabors that had a fixed size across all eccentricities, and for Gabors that scaled with retinal eccentricity. Only one retinal eccentricity across the 10 pair-wise comparisons showed a significant difference, and the variance in eccentricity from varying this stimulus property was smaller than between subject variance. Although there is a trend that larger stimuli raised the threshold, the overall effect was not significant (correcting for multiple comparisons) and so small in magnitude that we pooled the data for subject M in Figure 4(A).

We compared measurements from the marmoset acuity to that of the human and macaque. Figure 4(C) plots a psychophysical measurement of acuity in humans (solid black line, from Berkley et al., 1975) to the psychophysical measurement of marmoset acuity (solid green line). For the marmoset curve, we average the performance of subjects M and S with an additional measurement for central gaze taken from a previous study (Ordy and Samorajski, 1968). Instead of showing a clear inflection point in acuity leveling at around 5 degrees, the eccentricity at which cone density flattens in marmosets, marmoset acuity follows the same trend as human acuity staying roughly half of the value across eccentricity (dashed black line). In Figure 4(D), we also compared the psychophysical measurement of marmoset acuity (solid green line) and the measurement of the Nyquist limit (dotted green line, from Troilo et al., 1993) to macaque acuity (solid red line), the Nyquist limit from cone density (dotted red line), and the theoretical acuity limit based on P on and off retinal ganglion cell density (dotted black line) taken from data in Merigan and Katz, 1990. These comparisons show a similar pattern in which marmoset and macaque acuity deviates from the Nyquist limit of retinal cone densities at retinal eccentricities greater than 5–10 visual degrees.

One concern is that lapse rate in different sessions might have affected our threshold measurements. Lapse rate indicates the rate of failure for stimuli unrelated to their visibility, and could be from not attending to the visual display or because of difficulty performing the required response. We observed that lapse rate nominally increased for the second half of a behavioral session compared to the first half within individual subjects and eccentricities ($p < 0.05$, t-test). However, there were no significant changes in spatial frequency threshold across the first and second half of behavioral session ($p > 0.4$, t-test), and these changes in lapse rate were uncorrelated to changes in threshold ($r = 0.43$, $p = 0.21$). This suggests that estimation of threshold under the current methods (method of constant stimuli combined with parametric curve fits) is robust to higher lapse rates. The robustness to lapse rate will be critical for testing subjects without extensive previous training, for example, when using such tasks to evaluate if marmoset subjects require refractive correction.

DISCUSSION

This study measured a crucial feature of marmoset vision: sensitivity to spatial scale. Visual acuity determines what types of stimuli can reasonably be discriminated, and as such, is critical for design of stimuli in behavioral tasks to ensure the validity of the research. We tested marmoset acuity using a simple task that required minimal training. Subjects maintained fixation on a central point briefly as a vertical Gabor stimulus was displayed at an eccentric location, with reward given for a saccade to that location. We focused on characterizing acuity across the eccentricities from 1.5 to 12 degrees, a region that is of practical importance for studies using a head-fixed subject in visual neurophysiology. Our measurements compliment a prior behavioral study that estimated central marmoset acuity at close to 30 cycles per degree (Ordy and Samorajski, 1968). Together they place marmoset acuity at roughly half that of humans [Fig. 4(C)], which is consistent with the similar retinal cone density combined with the marmoset having an eye about half the size of a human. It should be noted that our acuity measurements are averaged across spatial locations, whether nasal, superior, inferior or temporal, and use only a single, vertical, Gabor orientation, both of which introduce some variance in acuity (e.g., Wilkinson et al., 2016). While providing a useful estimate of acuity, our measurements may differ from actual acuity of a specific axis and orientation. Nevertheless, these measurements provide a general guide for average detail that marmosets can see across the central visual field, which compares well to other primates, and is orders of magnitude above those observed in species without a specialized fovea such as the mouse (Histed et al., 2012).

The density of photoreceptors in the retina is a fundamental constraint to visual acuity. Previous studies examining the cone density in marmoset have calculated this theoretical limit, known as the Nyquist limit (Troilo et al., 1993), which when compared to humans and macaques suggests that marmosets could potentially have greater acuity at retinal eccentricities that exceed 5 degrees (Mitchell and Leopold, 2015). However, our psychophysical measurement of marmoset acuity indicates the marmoset visual system does not make use of these higher cone densities to increase the resolution of acuity. Marmoset acuity as a function of eccentricity, instead shows the same pattern as human acuity, scaled down by a factor of about 2 [Fig. 4(C)]. The lack of inflection in the psychophysical measurement of acuity may seem surprising given the higher peripheral cone density of the marmoset. However, this finding can be resolved by considering how those peripheral cone signals are pooled. In the macaque it has been shown that retinal P-ganglion cells pool across greater numbers of

12   *Nummela et al.*

photoreceptors in the periphery (Perry and Cowey, 1985), which could reduce the acuity of the retinal input to the rest of the visual system. This has been observed in macaques, in which the density of P-ganglion cells, and not cones, provided a better fit to behavioral acuity (Merigan and Katz, 1990). In Figure 4(D), we compare macaque acuity (solid red line) and Nyquist limits to cone (dotted red line) and P ganglion cell (dotted black line) densities taken from Merigan and Katz to marmoset acuity (solid green line) and Nyquist prediction from marmoset cone density (dotted green line, from Troilo et al., 1993). The Nyquist prediction for the marmoset shows a sharp inflection in slope past 5 degree eccentricity that is not evident for the Nyquist prediction of the macaque (dotted green versus dotted red lines). Nevertheless, the behavioral measurement of marmoset acuity deviates sharply from the Nyquist prediction, just like behavioral measurement of macaque acuity. For the macaque, this deviation can be explained by the higher convergence of cone photoreceptors onto P ganglion cells in the periphery. Our results suggest a similar convergence of cone photoreceptors in marmoset, which is consistent with an early study that reported peripheral pooling was greater in the periphery of the marmoset than in the macaque (Goodchild et al., 1996). Thus, while cone density may be greater in the marmoset periphery, with the greater pooling by retinal ganglion cells in the periphery this higher density is offset. These findings also help explain why the cortical magnification found at the level of visual cortex scales similarly to macaque and human (Chaplin et al., 2013).

One concern is that aliasing in the periphery may increase acuity sensitivity in the detection tasks (Thibos et al., 1996). This could in principle lead to supra-Nyquist detection in the periphery of vision (Williams and Coletta, 1987). We did not observe any signs of supra-Nyquist acuity thresholds in our peripheral data. This may reflect that our most peripheral locations were less eccentric than those of previous studies, or methodological differences such as our choice of display monitor. Of note, measurements of human acuity do not always reflect such peripheral aliasing either, as seen in Figure 4(C) by comparing those measurements using a detection task similar to our own (Berkley et al., 1975) against those measured recently using discrimination tasks of grating orientation that are robust to aliasing (Thibos et al., 1996). Thus while peripheral aliasing may be specific concern for certain test conditions, it does not appear prominent in our data nor could it account for our findings that peripheral acuity thresholds are significantly below the Nyquist limit.

Our findings also emphasize the importance of identifying refractive errors in marmosets prior to conducting visual experiments. One method to diagnose a subject is to perform an ophthalmological refraction, which requires substantial expertise. In subject M and S, we used an alternative set of diagnostics that can be performed using the same simple detection task. First, the presence of myopia can be diagnosed by comparing spatial frequency sensitivity for a fixed retinal eccentricity at two or more distances (such as 29 to 90 cm in the current study). A decrease in the spatial frequency threshold, as seen for subjects M and S [Fig. 2(B)], indicates nearsightedness. In performing this diagnostic, it is important to make sure that the display resolution is sufficient to present the desired stimulus, and this can be particularly challenging for near display distances. In our study, we found aliasing to be an issue with a standard monitor and had to repeat tests with a smaller display for near distances. Typically, 6 pixels per cycle is adequate sampling to ensure a minimal loss of effective stimulus contrast. Using a square wave grating cannot always alleviate this issue, as some light typically escapes from bright pixels into neighboring pixels, resulting in the loss of contrast when only 1 or 2 pixels are alternated in brightness. Second, to find an appropriate correction, we measured the spatial frequency threshold over a range of diopter correction strengths while the display distance remained at a far distance (90 cm). For subjects with myopia, spatial acuity will increase with larger corrections up to some point, where it will either flatten or begin to decline gradually due to the overcorrection [Fig. 2(D)]. Both of these diagnostics made use of the same simple detection task, which required only 1 to 5 training sessions, each an hour long in duration. In applying visual correction, one concern is that measurements at extreme eccentricities might be affected by differences in refractive error between central and peripheral locations (Wang et al., 1997). However, we find no evidence that this affects our results in the near periphery at 10 or 12 visual degrees, based on measurement of acuity threshold using a very near, 20 cm, display distance [Fig. 4(A), M* compared to M]. While most studies in macaque subjects use a display distance of 57 cm as a default, we would instead recommend closer display distances at or below 30 cm in marmoset subjects, unless other means are used to measure and correct myopia.

The incidence of myopia among marmosets raised in captivity is high, and could even be prevalent in natural habitats, and so will generally require correction to ensure the validity of vision studies. Unlike most primate species used in research, which are normally bred and raised in dedicated primate centers,

marmosets are often raised in smaller breeding colonies that may have limited access to distance viewing or natural lighting conditions, which may be a contributing factor. Although rare among macaques used in research, myopia has also been reported in a case study (Mitchell et al., 2014a). Previous studies with marmosets raised in captivity found that mild to severe myopia was common (Graham and Judge, 1999). Consistent with these findings, we observe that all marmosets tested in our study exhibited a significant myopia, ranging from -2 to -4 diopters. Several factors associated with rearing in laboratory conditions could contribute to myopia. One recent study using macaques indicated that indoor lighting conditions contributed to a much a higher incidence of myopia, and that better high light levels ($>10,000$ lux) reduced its incidence (Smith et al., 2012). Thus improvements to colony housing could reduce myopia among captive marmosets, which might have utility beyond their eye development but additionally might improve how they use distance vision in social settings. For example, in viewing other marmosets from a distance it is typically thought that they can make inferences about a conspecific's gaze direction, facial expression, or other social information (Miller et al., 2016). However, the development of such social monitoring could be impaired in colonies where the incidence of myopia is high. Regardless of these considerations, it is clear that some method to correct for refractive state is necessary prior to study of visual behavior in this species.

The common marmoset could provide a useful platform for examining spatial vision in disease models of human vision and across visual system development. Previous studies of macaques have related changes in visual receptive field properties at the level of visual cortex to measures of behavioral acuity early in life (for review Kiorpes, 2015). Simple behavioral tasks, including preferential looking, have been effective to measure acuity in macaque infants (Boothe et al., 1980, 1988; Movshon and Kiorpes, 1988). These studies show that receptive field properties of visual neurons near birth are much better than behavioral acuity at the same age (Kiorpes and Bassin, 2003). The development of mature acuity, present near 9 months of age, appears contingent on the development of higher stages of visual processing as well as reconfiguration of feedback connectivity (Kennedy and Burkhalter, 2004; Kiorpes et al., 2014). The marmoset could provide several advantages to complement these studies in the macaque. First, it is born at a relatively immature developmental stage compared to humans and macaques (Robinson and Dreher, 1990; Warner et al., 2012). As such

there is a window of opportunity to examine early development postnatally before mature receptive field properties are established. A recent study has shown interesting transitions between the retinopulvinar and retinocortical pathways for motion processing during this period (Warner et al., 2012). Second, the marmoset matures within a single year, making it possible to examine developmental changes in a considerably smaller time frame compared to macaques. In this study, we have introduced a set of simple behavioral methods that can be used to assess the quality of vision in the marmoset, and established baselines for spatial vision as a function of eccentricity in adults. These methods will be valuable to assess the development of acuity in the marmoset and to use this model for studies of ocular disease.

REFERENCES

Benavente-Perez A, Nour A, Troilo D. 2012. The effect of simultaneous negative and positive defocus on eye growth and development of refractive state in marmosets eye growth and development of refractive state. Invest Ophthalmol Vis Sci 53:6479–6487.

Berkley MA, Kitterle F, Watkins DW. 1975. Grating visibility as a function of orientation and retinal eccentricity. Vision Res 15:239–244.

Boothe RG, Kiorpes L, Williams RA, Teller DY. 1988. Operant measurements of contrast sensitivity in infant macaque monkeys during normal development. Vision Res 28:387–396.

Boothe RG, Williams RA, Kiorpes L, Teller DY. 1980. Development of contrast sensitivity in infant Macaca nemestrina monkeys. Science 208:1290–1292.

Brainard DH. 1997. The psychophysics toolbox. Spat Vis 10:433–436.

Chaplin TA, Yu HH, Rosa MG. 2013. Representation of the visual field in the primary visual area of the marmoset monkey: Magnification factors, point-image size, and proportionality to retinal ganglion cell density. J Comp Neurol 521:1001–1019.

Freitag FB, Pessoa DMA. 2012. Effect of luminosity on color discrimination of dichromatic marmosets (*Callithrix jacchus*). J Opt Soc Am A Opt Image Sci Vis 29: A216–A222.

Goodchild AK, Ghosh KK, Martin PR. 1996. Comparison of photoreceptor spatial density and ganglion cell morphology in the retina of human, macaque monkey, cat, and the marmoset *Callithrix jacchus*. J Comp Neurol 366: 55–75.

Graham B, Judge SJ. 1999. Normal development of refractive state and ocular component dimensions in the marmoset (*Callithrix jacchus*). Vision Res 39:177–187.

14   *Nummela et al.*

Histed MH, Carvalho LA, Maunsell JHR. 2012. Psycho-physical measurement of contrast sensitivity in the behaving mouse. J Neurophysiol 107:758–765.

Kennedy H, Burkhalter A. 2004. Ontogenesis of cortical connectivity. Vis Neurosci 1:146–158.

Kiorpes L. 2015. Visual development in primates: Neural mechanisms and critical periods. Dev Neurobiol 75:1080–1090.

Kiorpes L, Bassin SA. 2003. Development of contour inte-gration in macaque monkeys. Vis Neurosci 20:567–575.

Kiorpes L, Movshon A, Chaluppa W. 2014. Neuronal limi-tations on visual development in primates: Beyond striate cortex.

Kleiner M, Brainard D, Pelli D, Ingling A, Murray R, Broussard C. 2007. What's new in Psychtoolbox-3. Per-ception 36:1.

Lu T, Liang L, Wang X. 2001. Neural representations of temporally asymmetric stimuli in the auditory cortex of awake primates. J Neurophysiol 85:2364–2380.

Merigan WH, Katz LM. 1990. Spatial resolution across the macaque retina. Vision Res 30:985–991.

Miller CT, Freiwald WA, Leopold DA, Mitchell JF, Silva AC, Wang X. 2016. Marmosets: A neuroscientific model of human social behavior. Neuron 90:219–233.

Mitchell JF, Boisvert CJ, Reuter JD, Reynolds JH, Leblanc M. 2014a. Correction of refractive errors in rhesus maca-ques (*Macaca mulatta*) involved in visual research. Comp Med 64:300–308.

Mitchell JF, Leopold DA. 2015. The marmoset monkey as a model for visual neuroscience. Neurosci Res 93:20–46.

Mitchell JF, Reynolds JH, Miller CT. 2014b. Active vision in marmosets: A model system for visual neuroscience. J Neurosci 34:1183–1194.

Movshon JA, Kiorpes L. 1988. Analysis of the develop-ment of spatial contrast sensitivity in monkey and human infants. J Opt Soc Am A 5:2166–2172.

Nickla DL, Wildsoet CF, Troilo D. 2002. Diurnal rhythms in intraocular pressure, axial length, and choroidal thick-ness in a primate model of eye growth, the common mar-moset. Invest Ophthalmol Vis Sci 43:2519–2528.

Ordy JM, Samorajski T. 1968. Visual acuity and ERG-CFF in relation to the morphologic organization of the retina among diurnal and nocturnal primates. Vision Res 8:1205–1225.

Osmanski MS, Song X, Wang X. 2013. The role of har-monic resolvability in pitch perception in a vocal nonhu-man primate, the common marmoset (*Callithrixjacchus*). J Neurosci 33:9161–9168.

Pelli DG. 1997. The VideoToolbox software for visual psy-chophysics: Transforming numbers into movies. Spat Vis 10:437–442.

Perry VH, Cowey A. 1985. The ganglion cell and cone dis-tributions in the monkey's retina: Implications for central magnification factors. Vision Res 25:1795–1810.

Prins N, Kingdom FAA. 2009. Palamedes: Matlab routines for analyzing psychophysical data.

Rada JA, Nickla DL, Troilo D. 2000. Decreased proteogly-can synthesis associated with form deprivation myopia in mature primate eyes. Invest Ophthalmol Vis Sci 41:2050–2058.

Remington ED, Osmanski MS, Wang X. 2012. An operant conditioning method for studying auditory behaviors in marmoset monkeys. PLoS One 7:e47895.

Robinson SR, Dreher B. 1990. The visual pathways of eutherian mammals and marsupials develop according to a common timetable (part 1 of 2). Brain Behav Evol 36:177–186.

Smith EL, Hung LF, Huang J. 2012. Protective effects of high ambient lighting on the development of form-deprivation myopia in rhesus monkeys. Invest Ophthal-mol Vis Sci 53:421–428.

Thibos LN, Still DL, Bradley A. 1996. Characterization of spatial aliasing and contrast sensitivity in peripheral vision. Vision Res 36:249–258.

Troilo D, Judge SJ. 1993. Ocular development and visual deprivation myopia in the common marmoset (*Callithrix jacchus*). Vision Res 33:1311–1324.

Troilo D, Nickla DL. 2005. The response to visual form deprivation differs with age in marmosets. Invest Oph-thalmol Vis Sci 46:1873–1881.

Troilo D, Nickla DL, Mertz JR, Rada JAS. 2006. Change in the synthesis rates of ocular retinoic acid and scleral gly-cosaminoglycan during experimentally altered eye growth in marmosets. Invest Ophthalmol Vis Sci 47:1768–1777.

Troilo D, Nickla DL, Wildsoet CF. 2000a. Choroidal thick-ness changes during altered eye growth and refractive state in a primate. Invest Ophthalmol Vis Sci 41:1249–1258.

Troilo D, Nickla DL, Wildsoet CF. 2000b. Form depriva-tion myopia in mature common marmosets (*Callithrix jacchus*). Invest Ophthalmol Vis Sci 41:2043–2049.

Troilo D, Quinn N, Baker K. 2007. Accommodation and induced myopia inmarmosets. Vision Res 47:1228–1244.

Troilo D, Rowland HC, Judge SJ. 1993. Visual optics and retinal cone topography in the common marmoset (*Calli-thrix jacchus*). Vision Res 33:1301–1310.

Wang YZ, Thibos LN, Bradley A. 1997. Effects of refractive error on detection acuity and resolution acuity in peripher-al vision. Invest Ophthalmol Vis Sci 38:2134–2143.

Warner CE, Kwan WC, Bourne JA. 2012. The early matu-ration of visual cortical area MT is dependent on input from the retinorecipient medial portion of the inferior pulvinar. J Neurosci 32:17073–17085.

Whatham AR, Judge SJ. 2001. Compensatory changes in eye growth and refraction induced by daily wear of soft contact lenses in young marmosets. Vision Res 41:267–273.

Wilder HD, Grünert U, Lee BB, Martin PR. 1996. Topogra-phy of ganglion cells and photoreceptors in the retina of a New World monkey: The marmoset *Callithrix jacchus*. Vis Neurosci 13:335–352.

Wilkinson MO, Anderson RS, Bradley A, Thibos LN. 2016. Neural bandwidth of veridical perception across the visual field. J Vis 16:1–17.

Williams DR, Coletta NJ. 1987. Cone spacing and the visu-al resolution limit. J Opt Soc Am A 4:1514–1523.

AQ3

AQ1: Please confirm whether short title is OK as typeset.

AQ2: Please provide department/division for 1, 2, 4, 5 affiliations.

AQ3: Please provide complete details for references "Kiorpes L, Movshon A, Chaluppa W. 2014; Prins N, King-dom FAA. 2009."

AQ4: Please confirm that given names (red) and surnames/family names (green) have been identified correctly.

Please confirm that the funding sponsor list below was correctly extracted from your article: that it includes all funders and that the text has been matched to the correct FundRef Registry organization names. If a name was not found in the FundRef registry, it may be not the canonical name form or it may be a program name rather than an organization name or it may be an organization not yet included in FundRef Registry. If you know of another name form or a parent organization name for a not found item on this list below, please share that information.

FundRef name	FundRef Organization Name (Country)	FundRef DOI	Grant IDs
NIMH (to S.U.N., J.F.M.)	National Institute of Mental Health	10.13039/100000025	R0121MH104756-01
NIH (to S.U.N., J.F.M.)	National Institutes of Health	10.13039/100000002	U01-NS094330
NHMRC (Australia) Project	National Health and Medical Research Council	10.13039/501100000925	APP1083152